Plant Physiology and Biochemistry 210 (2024) 108609

Contents lists available at ScienceDirect

Plant Physiology and Biochemistry

journal homepage: www.elsevier.com/locate/plaphy

Integrated omics approach reveals the molecular pathways activated in tomato by *Kocuria rhizophila*, a soil plant growth-promoting bacterium

Antonio Mauceri [a,1], Guglielmo Puccio [b,c,1], Teresa Faddetta [d,1], Loredana Abbate [b], Giulia Polito [d], Ciro Caldiero [a], Giovanni Renzone [e], Margot Lo Pinto [d], Pasquale Alibrandi [f], Edoardo Vaccaro [f], Maria Rosa Abenavoli [a], Andrea Scaloni [e], Francesco Sunseri [a], Vincenzo Cavalieri [d], Antonio Palumbo Piccionello [d], Giuseppe Gallo [d,g], Francesco Mercati [b,*]

[a] University Mediterranea of Reggio Calabria, AGRARIA Department, Località Feo di Vito, 89122, Reggio Calabria, Italy
[b] National Research Council, Institute of Biosciences and Bioresources (IBBR), Via Ugo La Malfa 153, 90146, Palermo, Italy
[c] University of Palermo, SAAF Department, Viale Delle Scienze, 90128, Palermo, Italy
[d] University of Palermo, STEBICEF Department, Viale Delle Scienze, 90128, Palermo, Italy
[e] National Research Council, Proteomics, Metabolomics and Mass Spectrometry Laboratory (ISPAAM), Piazzale E. Fermi 1, 80055, Portici, (Napoli), Italy
[f] Mugavero Teresa S.A.S., Corso Umberto e Margherita 1B, 90018, Termini Imerese, (Palermo), Italy
[g] NBFC, National Biodiversity Future Center, Piazza Marina 61, 90133, Palermo, Italy

ARTICLE INFO

Keyworlds:
Plant growth-promoting bacteria
Omics
Soil actinomycete
Solanum lycopersicum
Weighted gene co-expression network analysis

ABSTRACT

Plant microbial biostimulants application has become a promising and eco-friendly agricultural strategy to improve crop yields, reducing chemical inputs for more sustainable cropping systems. The soil dwelling bacterium *Kocuria rhizophila* was previously characterized as Plant Growth Promoting Bacteria (PGPB) for its multiple PGP traits, such as indole-3-acetic acid production, phosphate solubilization capability and salt and drought stress tolerance. Here, we evaluated by a multi-omics approach, the PGP activity of *K. rhizophila* on tomato, revealing the molecular pathways by which it promotes plant growth. Transcriptomic analysis showed several up-regulated genes mainly related to amino acid metabolism, cell wall organization, lipid and secondary metabolism, together with a modulation in the DNA methylation profile, after PGPB inoculation. In agreement, proteins involved in photosynthesis, cell division, and plant growth were highly accumulated by *K. rhizophila*. Furthermore, "amino acid and peptides", "monosaccharides", and "TCA" classes of metabolites resulted the most affected by PGPB treatment, as well as dopamine, a catecholamine neurotransmitter mediating plant growth through S-adenosylmethionine decarboxylase (*SAMDC*), a gene enhancing the vegetative growth, up-regulated in tomato by *K. rhizophila* treatment. Interestingly, eight gene modules well correlated with differentially accumulated proteins (DAPs) and metabolites (DAMs), among which two modules showed the highest correlation with nine proteins, including a nucleoside diphosphate kinase, and cytosolic ascorbate peroxidase, as well as with several amino acids and metabolites involved in TCA cycle. Overall, our findings highlighted that sugars and amino acids, energy regulators, involved in tomato plant growth, were strongly modulated by the *K. rhizophila*-plant interaction.

1. Introduction

The very fast-growing world population and, consequently, the increasing demand for food require an intensification of crop production, which implies an excessive use of chemical inputs, often responsible of the environmental pollution and soil biodiversity loss (Bartucca et al., 2022). Tomato (*Solanum lycopersicum* L.) is one the most spread vegetables worldwide (FAOSTAT, 2020; https://www.fao.org/faostat/en) due to nutritional, health-promoting, and economical value of its fruits. The yield, size, shape, firmness, color, taste, and solid content improvement in tomato fruits represent important goals to increase the commercial value (Del Giudice et al., 2017). However, to

* Corresponding author.
E-mail address: francesco.mercati@cnr.it (F. Mercati).
[1] These authors have contributed equally to this work.

https://doi.org/10.1016/j.plaphy.2024.108609
Received 17 January 2024; Received in revised form 27 March 2024; Accepted 4 April 2024
Available online 13 April 2024

reach high product quality and yield as well as to increase the abiotic/biotic stresses resistance, an intensive application of chemical fertilizers is needed (Kalt, 2005). Therefore, it is mandatory to rethink a novel and more sustainable agriculture for tomato to preserve the environment – by reducing the usage of primary resources, such as water and land – and for a concurrent increase of crop yield as well as food nutritional value. In this respect, the use of Plant Biostimulants (PBs) may represent an eco-friendly and innovative tool for a sustainable agriculture, diminishing the environmental pressure of the cropping systems (Rouphael and Colla, 2020).

PBs, defined as fertilizers able to stimulate plant growth and development (EU, 2019; https://eur-lex.europa.eu/), can be classified as *i*) non-microbials, including bioactive substances (*e.g.*, protein hydrolyzates, seaweed extracts, and humic and fulvic acids), and *ii*) microbials, comprising Plant Growth Promoting Bacteria (PGPB) as well as arbuscular mycorrhizal fungi (AMF) (Du Jardin, 2015; Lombardi et al., 2020; Puccio et al., 2023). Among the beneficial effects of PGPB and AMF, worth mentioning is their ability to promote plant growth, nutrients use efficiency, tolerance to abiotic/biotic stresses, quality traits, and nutrients availability in soil and/or rhizosphere (Drobek Abd El-Daim et al., 2019; Guerrieri et al., 2021).

Currently, the use of PGPB-based biofertilizers pertains to the general strategy of plant microbiome modulation, which is considered as a valuable and alternative strategy to genetic manipulation and traditional breeding (Ray et al., 2020) for stimulating plant growth. In particular, PGPB, generally belonging to *Bacillus*, *Pseudomonas*, *Kocuria* and *Azospirillum* genus (Ruzzi and Aroca, 2015), promote diverse morpho-physiological, cellular and molecular processes that improve crop yield and quality, including: *i)* phytohormones, secondary metabolites, and/or volatile organic compounds (VOCs) production/regulation levels; *ii)* plant nutrients availability through nitrogen (N) fixation, phosphorus (P) solubilization and Fe supply, via production of organic acids, acid phosphatases, and siderophores; *iii)* photosynthetic efficiency improvement; *iv)* root growth and architecture modulation; *v)* resistance to abiotic and biotic stresses enhancement, such as drought and pathogens (De Andrade et al., 2023).

The genus *Kocuria,* belonging to the family *Micrococcaceae,* order *Actinomycetales*, includes *Kocuria rhizophila,* which is a Gram-positive bacterium, presenting coccoid cells grouped in pairs, chains, tetrads, cubical arrangements of eight, or irregular clusters (Stackebrandt et al., 1995). It is a soil dwelling bacterium, commonly used for antimicrobial testing and food preparations. Recently, studies performed on *K. rhizophila* strains revealed genes potentially involved in the biosynthesis of antifungal molecules, such as bacilysin and cycloserine (Guesmi et al., 2022) as well as the ability to improve maize plant growth under salt stress condition highlighting a mechanism preserving ion homeostasis and based on hormone synthesis and nutrient uptake regulation (H. Li et al., 2020). Thus, in consideration of the increasing interest on *K. rhizophila* strains as PGPB, another *K. rhizophila* strain has recently been characterized for multiple PGP traits such as indole-3-acetic acid production, phosphate solubilization capability and salt and drought stress tolerance and for its metabolome in the within of a collaborative research project, involving an academic–industrial consortium and aiming at the development of innovative biofertilizers (Faddetta et al., 2023).

Due to the complexity of PGPB-plant interaction, the molecular mechanisms underlying the beneficial effects of these microorganisms have not yet deeply elucidated, limiting their use in novel biofertilizer formulations for agronomic practices. Omics approach has been demonstrated as a valuable tool to elucidate plant molecular mechanisms and physiological processes affected by PGPB activity, as well as key components related to the protective action toward abiotic stresses (Lephatsi et al., 2021). In the present study, we have decoded metabolic pathways and molecular processes activated by *K. rhizophila*-based biofertilizer application in tomato. In particular, by using a multi-omics approach, leaf genes, proteins, and metabolites affected by PGPB treatment and involved in biological processes relevant for promoting tomato plant growth have been highlighted.

2. Materials and methods

2.1. Bacterial growth conditions

The *K. rhizophila* strain described and characterized in Faddetta et al. (2023) has been cultivated to obtain a biofertilizer improving plant growth. In particular, the strain was stored at −80 °C in a 20% (v/v) glycerol solution in Tryptone Soy Broth (Difco) from our laboratory collection (Faddetta et al., 2023). The strain was cultivated on agar plates containing Luria Bertani (LB) growth medium at 30 °C overnight to obtain single colonies. The biomass of a single colony was suspended in a 0.85% NaCl solution and then inoculated into 10 mL tubes containing 2 mL of LB broth medium and incubated at 28 °C and 160 rpm overnight. Subsequently, 0.75 mL of the culture (1.5% v/v) is transferred into 50 mL of R5A medium contained in 250 mL flask and incubated at 28 °C and 160 rpm overnight. Then, 12 mL (1.5% v/v) of this culture is transferred into a 1 L fermenter (Applikon Ez Control, Getinge) containing 0.8 L of R5A medium. The *K. rhizophila* was performed at pH 6.8 and 28 °C, for 24 h, with an aeration rate of 1.0 air volume/working volume/min and agitation rate of 250–350 rpm, to ensure that the dissolved oxygen in the solution was ≥30%. Fermentation broth was collected in sterile 500 mL bottles and stored at −80 °C until use. Cell concentration was measured spectrophotometrically (OD_{600}) and using cultivation broth serial dilutions for colony forming unit (CFU) counting on LB agar plates after overnight incubation at 30 °C.

2.2. Plant material and treatment

Four-weeks tomato plants (*S. lycopersicum* L.) of uniform size were transplanted in plastic pots (Ø 22 cm, h 22 cm, 7 L) filled with coconut fiber and placed in a growth-controlled chamber (25 ± 2 °C, 65–75% relative humidity, 12 h of daylight with a light intensity 18–20 kilolux). After transplanting, a PGPB treatment was carried out on plantlets by drenching with 100 mL of *K. rhizophila* cultivation broth dilution, containing 10^7 CFU/mL (Faddetta et al., 2023; referred as K plants), while the same amount of distilled water was used for the control (Ct), following a randomized design. A second treatment was carried out after 14 days. All the tomato plants (30 for each thesis) were fertirrigated with a standard nutrient solution (50 mg HNO_3 65%, 242 mg $Ca(NO_3)_2$, 210 mg KNO_3, 147 mg $Mg(NO_3)_2$, 38 mg NH_4NO_3, 88 mg KH_2PO_4, and microelements including Fe-EDTA) three times a day. Tissues (shoot and root) of Ct and K plants for each treatment were harvested at 14 (T1) and 42 (T2) days from the first *K. rhizophila* inoculation (Fig. S1) and stored at −80 °C until use. Shoot, consisting of a bulk of three branches at the third node, and the entire root were collected for each plant. Three biological replicates (each consisting of three plants bulked), for each sampling time and treatment, were freeze-dried and ground to a fine powder. Aliquots of the same material were used for the multi-omics analysis. To evaluate the tissue (shoot and/or root) to investigate in depth, the PGPB effect on tomato plant growth was preliminary assessed by evaluating fresh and dry weight of Ct and K plants, at each sampling time for both tissues. Tukey's test ($p < 0.05$) was applied to assay the significance among treatments.

2.3. Transcriptomic analysis

Leaf total RNA was isolated using a NucleoSpin RNA Plant (Macherey-Nagel GmbH & Co. KG, 52,355 Düren, Germany) and treated with RNase-free DNase. RNA integrity was assessed using an Agilent Bioanalyzer RNA nanochip (Agilent, Wilmington, DE). Sequence libraries were prepared as already reported (Puccio et al., 2022). Quality, quantity, and insert size distribution were assessed using an Agilent Bioanalyzer DNA 1000 chip. Sequence libraries were pooled in

equimolar concentration and analyzed on an Illumina NextSeq500 generating 2 × 100 nt paired end (PE) reads. The generated reads were deposited in the NCBI (National Center for Biotechnology Information) repository with dataset identifier PRJNA1058288.

Raw reads obtained from all samples were assessed for quality by FastQC v0.11.8 (https://www.bioinformatics.babraham.ac.uk/projects/fastqc/). Adapter was removed and the trimming was performed using Trimmomatic v0.38.0 (http://www.usadellab.org/cms/?page=trimmomatic). Reads were filtered by length and only those longer than 20 bp were selected. The filtered reads were mapped on the latest available tomato reference genome (SL4.0) (https://solgenomics.net/organism/Solanum_lycopersicum/genome) using RNA STAR v2.7.8a (https://code.google.com/archive/p/rna-star/). Transcript quantification was performed using htseq-count v0.9.1 (https://htseq.readthedocs.io/en/latest/). All the sampling times (T1, and T2) within and between each thesis (Ct and K) were compared to identify the Differentially Expressed Genes (DEGs) (log_2FoldChange $\geq \pm$ 1.0 and Padj <0.05). DEGs isolation, Principal Component Analysis (PCA), and heatmap visualization were carried out by Deseq2 (http://www.bioconductor.org/packages/release/bioc/html/DESeq2.html) and ClustVis (https://biit.cs.ut.ee/clustvis/), respectively, using default settings. Gene ontology (GO) enrichment analysis of specific gene functions across treatments was assessed with AgriGOv2.0 software (http://systemsbiology.cau.edu.cn/agriGOv2/) by using *S. lycopersicum* Transcript ID (ITA4.0 version). Finally, the MapMan tool (http://gabi.rzpd.de/projects/MapMan/) was used to link specific metabolic pathways to isolated DEGs.

2.4. RT-qPCR analysis

Reverse transcription quantitative PCR (RT-qPCR) was performed to target and validate the transcript abundance of candidate genes (primer sequences are listed in Table S1), using the *actin7-like* as housekeeping gene, following a procedure previously described (La Rocca et al., 2021). RT-qPCR experiments were performed on three biological replicates for each thesis, and all reactions were run in technical triplicate on a Step OnePlus Real-Time PCR System (Thermo Fisher Scientific) using SYBR Green detection chemistry. Relative expression levels were calculated as described in Livak and Schmittgen (2001).

2.5. DNA methylation level

Global DNA methylation levels, referred to as the total level of 5-methylcytosine (5-meC) content in a sample, were quantified using MethylFlash Methylated DNA Quantification kit (Epigentek), as previously described (Faddetta et al., 2023). Briefly, 100 ng of genomic DNA samples were bound to an ELISA plate and fluorescently labeled for 5-meC presence using specific antibodies. Each sample was run in duplicate along with internal controls provided by the kit, and the corresponding optical density (OD) intensity was measured based on the amount of 5-meC absorbance at 450 nm. The slope of the standard curve generated by positive controls was determined using linear regression and used to identify the total 5-meC amount of each sample. The percentage of global DNA methylation was then calculated as a ratio of sample OD relative to the OD of positive controls, after subtracting the negative control OD values. Data are presented as a mean ± standard error (SE). The significance among treatments was evaluated by Tukey's test ($p < 0.05$).

2.6. Proteomic analysis

Whole protein extracts from 100 mg of tomato leaves were obtained as already described in Faddetta et al. (2018) with modifications. In particular, leaf samples were washed five times with 1 mL 10% v/v TCA/acetone, one with 0.1 M ammonium acetate/methanol, one with acetone, and twice with 1 mL of extraction buffer (10 mM Tris–HCl pH 7.5, 5 mM EDTA, 1 mM DTT, 0.5 mM PMSF, 5 μg/mL leucopeptin, 7 μg/mL pepstatin, 4 μg/mL benzamidine) by vortexing, before their centrifugation (15,000×*g*, 10 min, at 4 °C). Cells were disrupted by sonication on ice (8 times, 15 s at setting 4 with 10 s break in-between each pulse, Vibra Cell, USA) in 1 mL of extraction buffer containing 0.3% w/v sodium dodecylsulfate. The samples were boiled for 5 min, rapidly cooled down on ice, and then treated with DNase (100 μg/mL) and RNase (50 μg/mL) in ice, for 15 min. Cell debris and non-broken cells were separated by centrifugation (15,000×*g*, for 15 min, at 4 °C). Protein extracts were treated with 1 vol of phenol/chloroform/isoamyl alcohol (25:24:1 v/v/v; Sigma-Aldrich) for 5 min, at room temperature, mixing by vortex. After centrifugation (15,000×*g*, 5 min, at 4 °C), protein extracts were recovered from the interface and the organic phase, after discharging the aqueous counterpart. Proteins were precipitated with 0.1 M ammonium acetate/methanol, at −20 °C, overnight, and protein precipitates were recovered by centrifugation (15,000×*g*, 10 min, at 4 °C). Protein pellets were washed with 1 mL of methanol, then with 1 mL of acetone, and finally dried under vacuum. They were dissolved in 8 M urea, 50 mM triethylammonium bicarbonate, 1% w/v protease inhibitor mix (Sigma-Aldrich), pH 8.5, and treated as previously reported (Rosina et al., 2022). Protein concentration was assessed with the BCA protein assay (Pierce, USA). Equal amounts of protein samples (100 μg) were reduced with 5 μL of 200 mM tris (2-carboxyethyl) phosphine for 60 min, at 55 °C, and then alkylated with iodoacetamide, precipitated with cold acetone, pelleted by centrifugation and then vacuum dried (Rosina et al., 2022).

Each protein sample was independently digested with trypsin (enzyme to protein ratio, 1:50), at 37 °C, overnight. Resulting peptides were labeled with TMT10plex Isobaric Label reagent kit (Thermo-Fisher Scientific). For a set of comparative experiments, tagged peptides were mixed in equal molar ratios (1:1) and dried under vacuum. Pooled TMT-labeled peptide mixtures were solved in 0.1% v/v trifluoroacetic acid and fractionated with a high pH reversed-phase microcolumn (ThermoFisher Scientific) into eight fractions, which were analyzed on a nanoLC-ESI-Q-Orbitrap-MS/MS platform consisting of a HPLC UltiMate™ 3000 RSLCnano System coupled to a Q-ExactivePlus mass spectrometer through a Nanospray Flex Ion Source (ThermoFisher Scientific). Peptides were loaded onto an Acclaim™ PepMap™ RSLC C18 column (150 mm × 75 μm ID, 2 μm particles, 100 Å pore size) (ThermoFisher Scientific) and eluted with a gradient of solvent B (19.92/80/0.08 [v/v/v] water/acetonitrile/formic acid) in solvent A (99.9/0.1 [v/v] water/formic acid), at a flow rate of 300 nL/min. Gradient and mass spectrometer settings were already reported (Rosina et al., 2022).

Raw data MS files for three technical replicates of each fraction were merged for protein identification and relative protein quantification into Proteome Discoverer (PD) software v. 2.4 (Thermo Scientific), allowing a database search by Mascot algorithm v. 2.4.2 (Matrix Science, UK) using the following criteria: UniProtKB protein database (*S. lycopersicum*, 36,951 protein sequences; *K. rhizophila*, 2352 protein sequences, 03/2022), including the most common protein contaminants; carbamidomethylation of Cys and TMT10plex modification of lysine and peptide N-terminus were set as fixed modifications; all other settings were previously reported (Rosina et al., 2022). Protein candidates were considered as confidently identified when assigned based on at least two sequenced peptide spectra matchings (PSMs) with an individual Mascot Score ≥25. For relative protein quantification, PD software calculated abundance ratios between experimental samples from the ratios of TMT reporter ion intensities in the MS/MS spectra from raw datasets. Results were filtered to a false discovery rate of 1%. Proteomic data were deposited to the ProteomeXchange consortium (https://www.proteomexchange.org/) within the PRIDE partner repository with the dataset identifier PXD038137.

Differentially Abundant Proteins (DAPs) were selected for each pairwise comparisons using a p-value threshold of 0.05. Ids were converted to ensembl genomic ids using uniprot id mapper (https://www.uniprot.org/id-mapping). The entire set of DAPs was used for a GO

enrichment analysis using DAVID (https://david.ncifcrf.gov/home.jsp). Significantly enriched GO terms (FDR <0.05) were fed to Cytoscape to evaluate an enrichment map. KEGG enrichment analysis was performed using the Shinygo online tool (http://bioinformatics.sdstate.edu/go74/) and visulized using ggplot2 R package (https://ggplot2.tidyverse.org/).

2.7. Metabolomic analysis

Leaf samples for HPLC were prepared suspending 100 mg of freeze-dried material with MeOH (5 mL) and sonicating them for 1 h. The solvent was filtered and injected. HPLC/MS analysis was performed on an Agilent 1260 Infinity using LC-MS grade water and acetonitrile, and analytical-grade formic acid. A reversed-phase Phenomenex Luna C18 (2) column (150 mm × 4.6 mm, 3 μm particles) with a Phenomenex C18 security guard column (4 × 3 mm) was used. Injection volume was 25 μL. The eluate was monitored through Mass Total Ion Count (MS TIC) and UV (270 nm). Mass spectra were obtained with an Agilent 6540 UHD accurate-mass Quadrupole-Time of flight (Q-TOF) spectrometer equipped with a Dual AJS Electrospray Ionization (ESI) source working in positive or negative mode. N_2 was used as desolvation gas at 300 °C and a flow rate of 8 L/min. The nebulizer was set to 45 psig. The sheath gas temperature was set at 400 °C and a flow rate of 12 L/min. Potentials of 2.6 kV and 3.2 kV were used on the capillary for negative and positive ion mode, respectively. The fragmentor was set to 75 V. MS spectra were recorded in the *m/z* range 150–1000.

Metabolomic data were normalized and analyzed using MetaboAnalyst 4.0 (https://www.metaboanalyst.ca/), highlighting qualitative and quantitative variations of metabolites between both treatments and times. The differential metabolites in the K *vs*. Ct comparison at each time were screened by combining the Fold Change (FC; ≥1) and *T*-tests ($p < 0.05$). Metabolite pathways analysis was developed, and the paths with $p < 0.05$ and higher impact value (≥0.5) were considered statistically significant.

2.8. Integrated weighted gene co-expression network analysis by using multi-omics data

A weighted gene co-expression network analysis (WGCNA) was performed on the DESeq2 variance stabilizing transformed (VST) expression data of the previously identified DEGs using the WGCNA package in R language (https://CRAN.R-project.org/package=WGCNA). WGCNA soft threshold power parameters were defined based on the approximate preconditions of the unscaled topology and the cut-off criteria of Edge Threshold = 0.80. All the variable sets were used to build the weighted gene co-expression network and visualize the gene modules using WGCNA. Topological overlap matrix (TOM) and the corresponding dissimilarity (1-TOM) were calculated using the adjacency matrix. After a hierarchical clustering, the highly correlated genes were included in the same module by using the Dynamic Tree Cut algorithm (minimum module size = 10). This analysis identified modules representing highly interconnected genes represented by different color and defined as Module Eigengene (ME; threshold = 11). Multi-omics relationships were presented by a heatmap based on Pearson's correlation between module expression profile (ME) and the other -omics variables (proteins and metabolites) with the aim to identify module membership (MM). The chromatic scale (red, blue) represents the strength of the correlation, while each box includes the correlation *p*-value. To identify the hub genes network, the VisANT 5.53 tool was used (http://www.visantnet.org/visantnet.html).

3. Results

3.1. Effects of K. rhizophila treatment on tomato plant growth

The K and Ct tomato plants grown in a phytotron were sampled at T1 and T2 (Fig. S1). The K plants showed a significant increase ($p < 0.05$) in both fresh and dry weight of shoot at each sampling time compared to the control (Ct) (Fig. 1A; Fig. S2). By contrast, in K root, a significant increase in fresh weight was recorded only at T1 ($p < 0.05$), while any changes were measured in dry weight at T1 and in both fresh and dry weight at T2 (data not shown). These results suggested to focus our attention on shoot, for dissecting the molecular mechanisms and metabolic pathways activated in tomato plants following the action of *K. rhizophila*.

3.2. Differentially expressed genes in K. rhizophila-treated plants

The leaf transcriptomic profiles of K and Ct tomato plants at T1 and T2 were compared. The transcriptomic statistical analysis was performed on the whole differentially expressed gene (DEG) dataset (Table S2). The PCA highlighted the main source of variation between the inoculated samples (K-T1 *vs*. K-T2); conversely, Ct-T1 and Ct-T2 resulted very closed and distinguished from the inoculated samples. PC1 and PC2 explained 25.8% and 18.5% of the total variance, respectively (Fig. S3). Accordingly, the correlation coefficient heatmap of the expression patterns for the most variable genes displayed a clear separation between K and Ct plants, with K-T2 more distant from the controls (Ct-T1 and Ct-T2) compared to K-T1 (Fig. 1B). A two pairwise comparison of DEGs between K and Ct plants showed: 615 and 608 up- and down-regulated DEGs in K-T1 *vs.* Ct-T1; 912 and 1096 up- and down-regulated DEGs in K-T2 *vs.* Ct-T2; 321 and 312 up- and down-regulated DEGs in Ct-T2 *vs.* Ct-T1; 1272 and 1339 up- and down-regulated DEGs in K-T2 *vs*. K-T1 (Fig. 1C). A significant lower number (87) of unique DEGs was identified in the Ct-T2 *vs.* Ct-T1 comparison (Fig. 1D). By contrast, the highest number of unique DEGs was observed in the K-T2 *vs*. K-T1 (839), K-T2 *vs*. Ct-T2 (535) and K-T1 *vs*. Ct-T1 (297) comparisons (Fig. 1D). Furthermore, 179 DEGs were shared in the comparisons that included K-T2, while 172 DEGs were identified in both K *vs*. Ct comparisons, regardless sampling time (Fig. 1D). Finally, 95 DEGs were common to all pairwise comparisons.

To validate the transcriptomic results, nine randomly chosen key isolated DEGs (Table S1) were tested by RT-qPCR. Overall, their relative gene expression trend was comparable to that resulting from RNASeq data (Fig. S4).

3.3. Enriched GO terms for DEGs and methylation profiles associated with K. rhizophila treatment

To obtain more information on the molecular mechanisms induced by *K. rhizophila* on tomato plants, a Gene Ontology (GO) enrichment analysis, including up- and down-regulated genes distinctly, was performed for the main three GO categories (Molecular Function, MF; Cellular Component, CC; Biological Process, BP) (Fig. 2A; Fig. S5; Table S3). The GO functional annotation results highlighted that, in K plants, the up-regulated DEGs belonging to BP (FDR <0.05) were mainly related to *i)* response to external factors or involved in the host-interaction (such as "response to stress", "cellular response to stimulus", and "cellular response to stress"), *ii)* catabolic processes (*e.g.* "macromolecule catabolic process" or "polysaccharide catabolic process"), *iii)* transport (like "intercellular transport" or "plasmodesmata-mediated intercellular transport"), and *iv)* steroid and sterol metabolic process. Among significantly enriched GO terms for down-regulated genes, many BP categories were included in photosynthetic pathways (Fig. 2A; Table S3), and metabolism processes (such as "tetrapyrrole metabolic process", "serine family amino acid metabolic process", "flavonoid metabolic process", "flavonoid biosynthesis process", and "small molecule metabolic process"). DEG metabolic categories within these groups differed in response to *K. rhizophila* treatment (Fig. 2A; Table S3), highlighting a variation of DEGs number and their biological function between K and Ct samples during time.

MapMan analysis showed that *K. rhizophila*-specific DEGs were mainly related to amino acid metabolism, cell wall organization, lipid

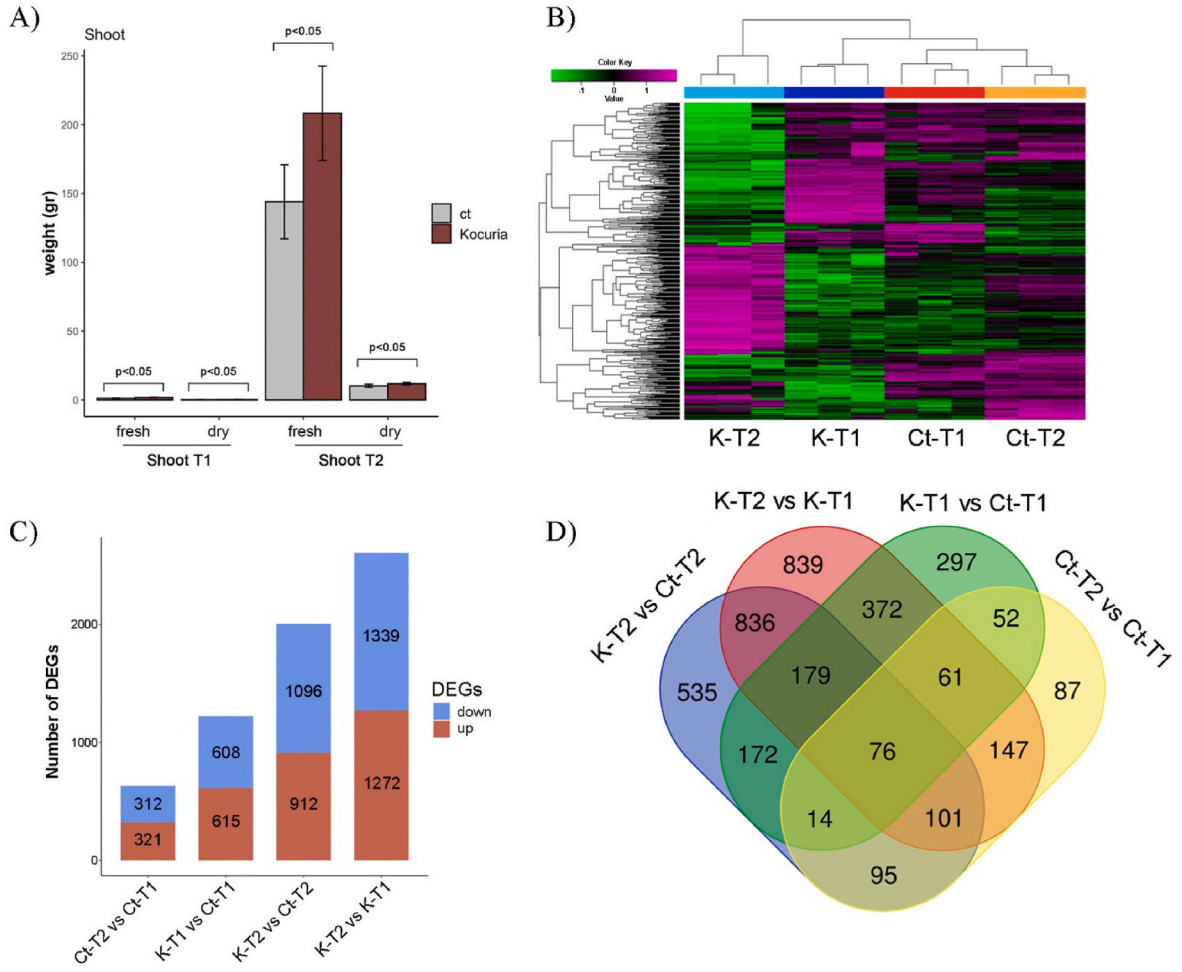

Fig. 1. Morphological and transcriptomic comparison of *K. rhizophila*-inoculated (K) and non-inoculated (Ct) tomato plants. **A)** Morphological effects (fresh and dry shoot weight) of *K. rhizophila* treatment on tomato plants. The significant differences between K and Ct samples (based on the Student's *t*-test) are indicated ($P < 0.05$). **B)** Heatmap expression pattern of the five hundred most variable genes detected in leaves of K and Ct plants at each time point (T1 and T2). **C)** Number of differentially expressed genes (DEGs) detected between each comparison. **D)** Venn diagram showing the number of unique and common Differentially Expressed Genes (DEGs) for each comparison.

and secondary metabolism (Fig. 2B). C1-metabolism, linked to long-term development, light reaction, nucleotide metabolism, oxidative pentose phosphate, and tricarboxylic acid cycle (TCA) were also influenced by *K. rhizophila* treatment (Fig. 2B; Table S3). Functional annotation highlighted an increase in the expression level of several genes related to plant growth and development in treated plants. Indeed, few genes (Solyc09G090680.3.1, Solyc03G005690.3.1 and Solyc06G083750.3.1) related to plant development or stress responses in the "host interaction" category were identified (Table S3), such as those coding a cysteine-rich repeat secretory protein and two plasmodesmal proteins (PDs), which were also included in the "plasmodesmata-mediated intercellular transport" category. In the "catabolic processes" category, an over-expression of genes associated with several aspartic proteases (APs, *e.g.*, Solyc07g006470.1.1, Solyc08g067100.2.1 and Solyc06g069220.1.1) was observed, involved in plant growth and development (Cao et al., 2019). Regarding "steroid and sterol metabolic process" category, genes coding allene oxide synthases (AOS; Solyc04g079730.1.1 and Solyc11g069800.1.1), which favor production of the jasmonic acid (JA) precursor allene oxide, resulted up-regulated in K plants together with S-adenosylmethionine decarboxylase (SAMDC; Solyc06g054460.1.1), included in the "amine metabolic process" category and having a key role in plant growth and development (Tassoni et al., 2007). A similar expression profile was observed for the gene coding inositol transporter (Solyc12g099070.1.1), identified in the "inorganic anion transport" category, and related to important plant signaling pathways (Zhou et al., 2022).

In contrast, several genes translating proteins involved in Calvin cycle, photosystem I and II were down-regulated after *K. rhizophila* treatment, such as geranylgeranyl reductase gene (GGR; Solyc03g115980.1.1), included in both "chlorophyll metabolic process" and "tetrapyrrole metabolic process" categories. Regarding "flavonoid metabolic process" category, genes coding enzymes catalyzing the formation of vinorine (vinorine synthase; Solyc07g006670.1.1, Solyc07g006680.1.1 and Solyc12g096800.1.1), a precursor of the monoterpenoid indole alkaloid related to stone cell development, and agmatine coumaroyl-transferases (Solyc11g071470.1.1 and Solyc11g071480.1.1) showed a lower expression in K plants compared to Ct ones.

The different expression pattern was detected between K and Ct samples agreed with the global DNA methylation profiling recorded. As expected, significant differences in the leaf methylation pattern were observed between treatments, with higher levels of methylation ($p < 0.05$) in K plants at both sampling times (Fig. S6).

3.4. Differentially accumulated proteins in *K. rhizophila*-treated plants and their KEGG ontology

Proteomic analysis of K and Ct leaves at T1 and T2 identified proteins

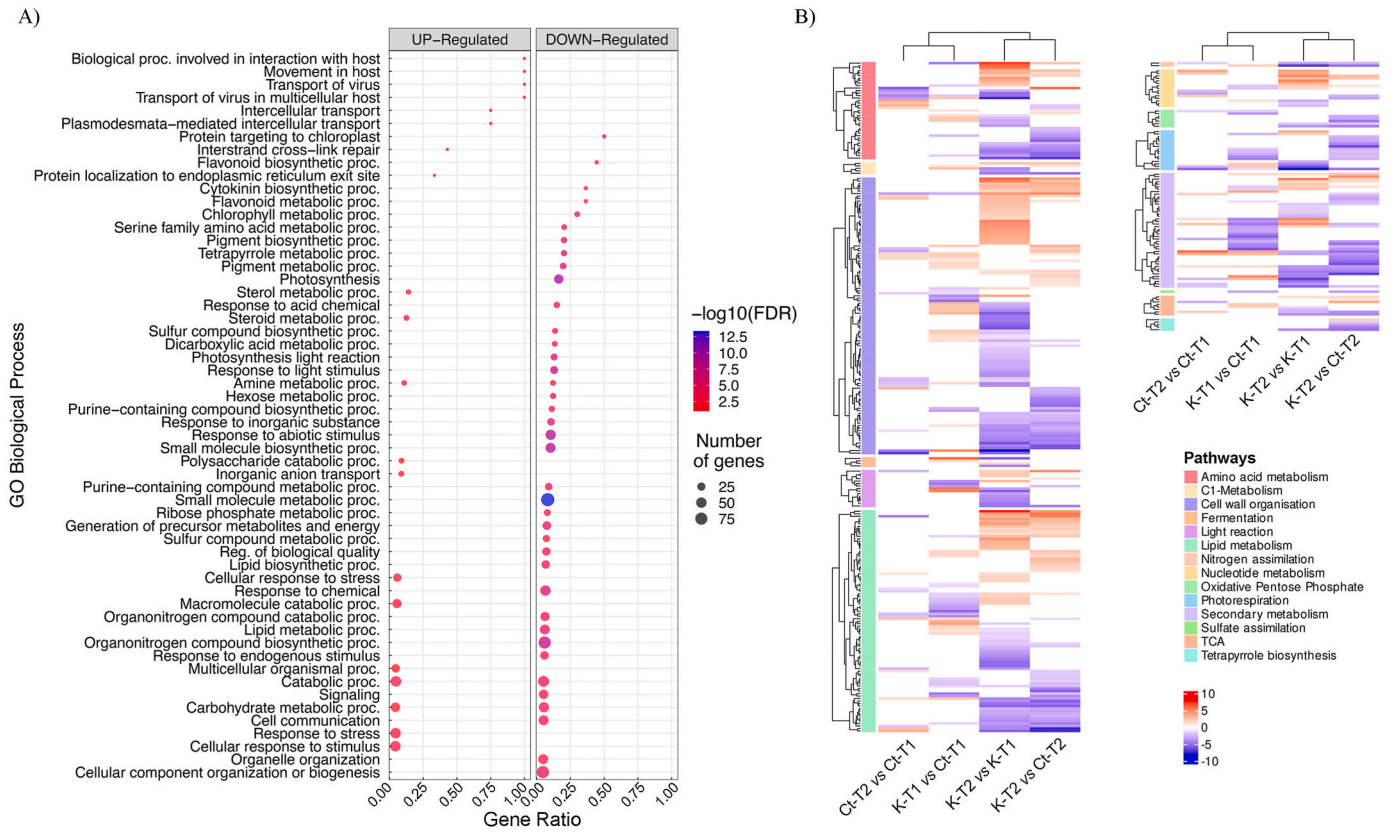

Fig. 2. A) Gene ontology (GO) enrichment analysis for the Biological Process (BP) category of up- and down-regulated genes detected in leaves of *K. rhizophila*-inoculated (K) and non-inoculated (Ct) tomato plants; those regarding the Molecular Function (MF) and Cellular Component (CC) categories are included in Fig. S7. **B)** Differentially Expressed Genes (DEGs) related to the main pathways extracted between each comparison.

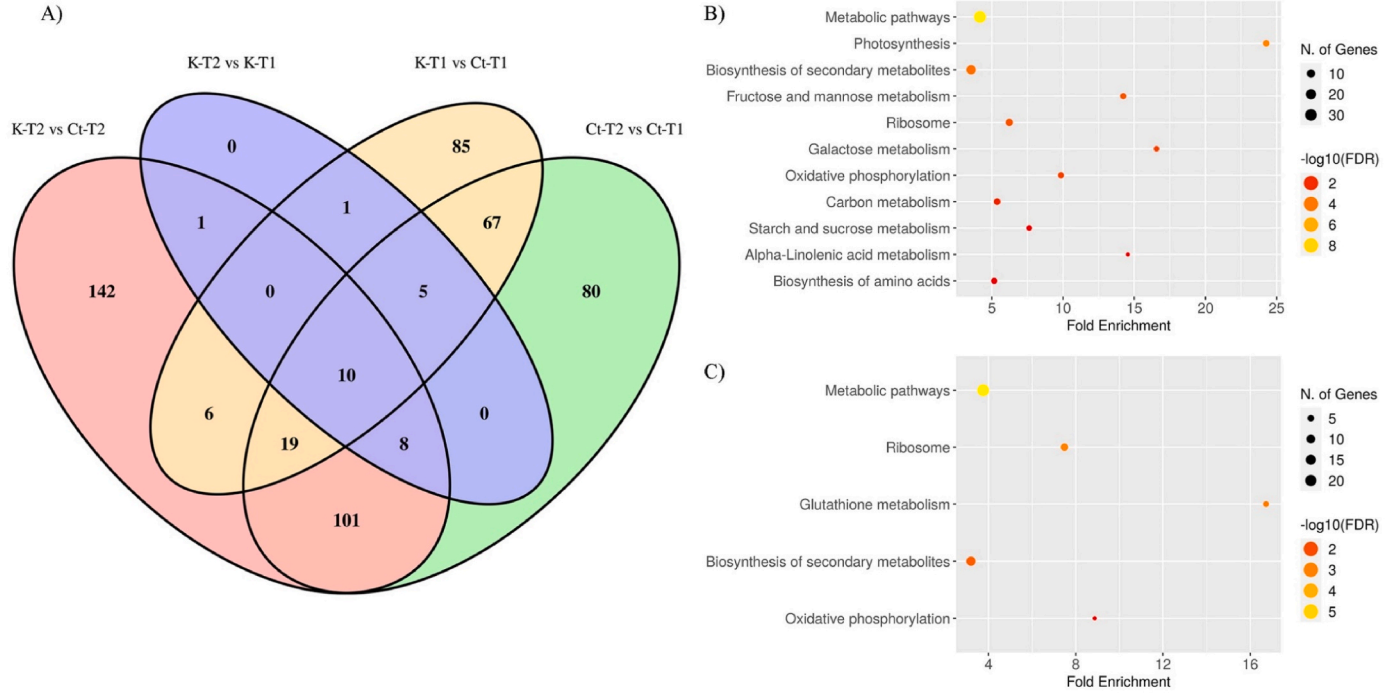

Fig. 3. Proteomics analysis of leaves from *K. rhizophila*-inoculated (K) and non-inoculated (Ct) tomato plants. **A)** Venn diagram of Differentially Accumulated Proteins (DAPs) between each comparison group (Ct-T2 *vs.* Ct-T1; K-T2 *vs.* K-T1; K-T1 *vs.* Ct-T1; K-T2 *vs.* Ct-T2). **B)** Kyoto Encyclopedia of Genes and Genomes (KEGG) analysis of DAPs resulting from comparison of K and Ct tomato plants at T1, and **C)** T2.

associated with 3177 non-redundant plant sequence entries. Overall, 193 and 287 Differentially Accumulated Proteins (DAPs) were identified in K-T1 *vs*. Ct-T1 and K-T2 *vs*. Ct-T2 comparisons, respectively (Table S4). Among these, 85 and 142 DAPs were uniquely identified in the K *vs.* Ct comparisons at T1 and T2, respectively (Fig. 3A). Along time, 80 proteins showed a different representation in Ct samples, while any DAPs were identified in the K-T2 *vs.* K-T1 comparison, and consequently any DAPs were shared between K and Ct samples (Fig. 3A).

According to their sequence identity or similarity to proteins from other species, GO analysis classified DAPs into 120 functional groups belonging to BP, CC, and MF categories (Table S5). Among the enriched BP categories, several groups of DAPs were involved in response to oxidative stress, transport, and metabolic processes. Among them, many categories related to photosystem ("plastid", "thylakoid membrane", "thylakoid", "chloroplast stoma", "respiratory chain") and cell organelles were identified in both CC and MF categories (Fig. S7). In addition, several categories involved in carbohydrate and amino acid metabolism were also extracted.

KEGG analysis of DAPs in the K *vs.* Ct comparisons identified 11 and 5 main categories at T1 and T2, respectively (Fig. 3B; Fig. 3C; Table S6). KEGGs isolated at T2 were also observed at T1, showing comparable fold enrichment values, except for "glutathione metabolism" (with a fold enrichment value of 16.72) (Table S6).

Among DAPs isolated (Table S4), several proteins involved in photosynthesis, cell division, and plant growth showed higher levels in *K. rhizophila*-inoculated plants. This is the case of a photosynthetic NDH subcomplex protein (Solyc05G007780.3), three photosystem II reaction center Psb family proteins (Solyc06g065490.3; Solyc08g067840.3; Solyc09g064500.3), photosystem I reaction center subunit IV and V family proteins (Solyc07g066150.1 and Solyc09g063130.3), a thylakoid membrane phosphoprotein (Solyc10g005050.3), a chlorophyll *a-b* binding protein (Solyc12g011450.2), and ATP synthase delta-subunit protein (Solyc12g056830.1). A similar quantitative trend was observed for succinyl-CoA ligase (SCoAL) involved in TCA cycle, two hexokinases involved in plant development and stress resistance, namely HXK1 (Solyc03g121070.3) and HXK4 (Solyc04G081400.3), two enolases (Solyc06G076650; Solyc10g085555.1.1) affecting plant growth and metabolism, an alpha-ketoglutarate dehydrogenase E2 (Solyc12G005080.2) involved in the basal immune response against bacterial in tomato (Ma et al., 2020), a cytosolic ascorbate peroxidase (APX1; Solyc06g005160.3) able to mitigate oxidative stress, cytochrome *c* oxidase subunit Vb (Solyc12G042900.2) and two phosphofructokinases (PFKs) (Solyc12G095880.2; Solyc07g045160.3), having a role in the cell division (Beauvoit et al., 2014). Finally, *K. rhizophila* treatment

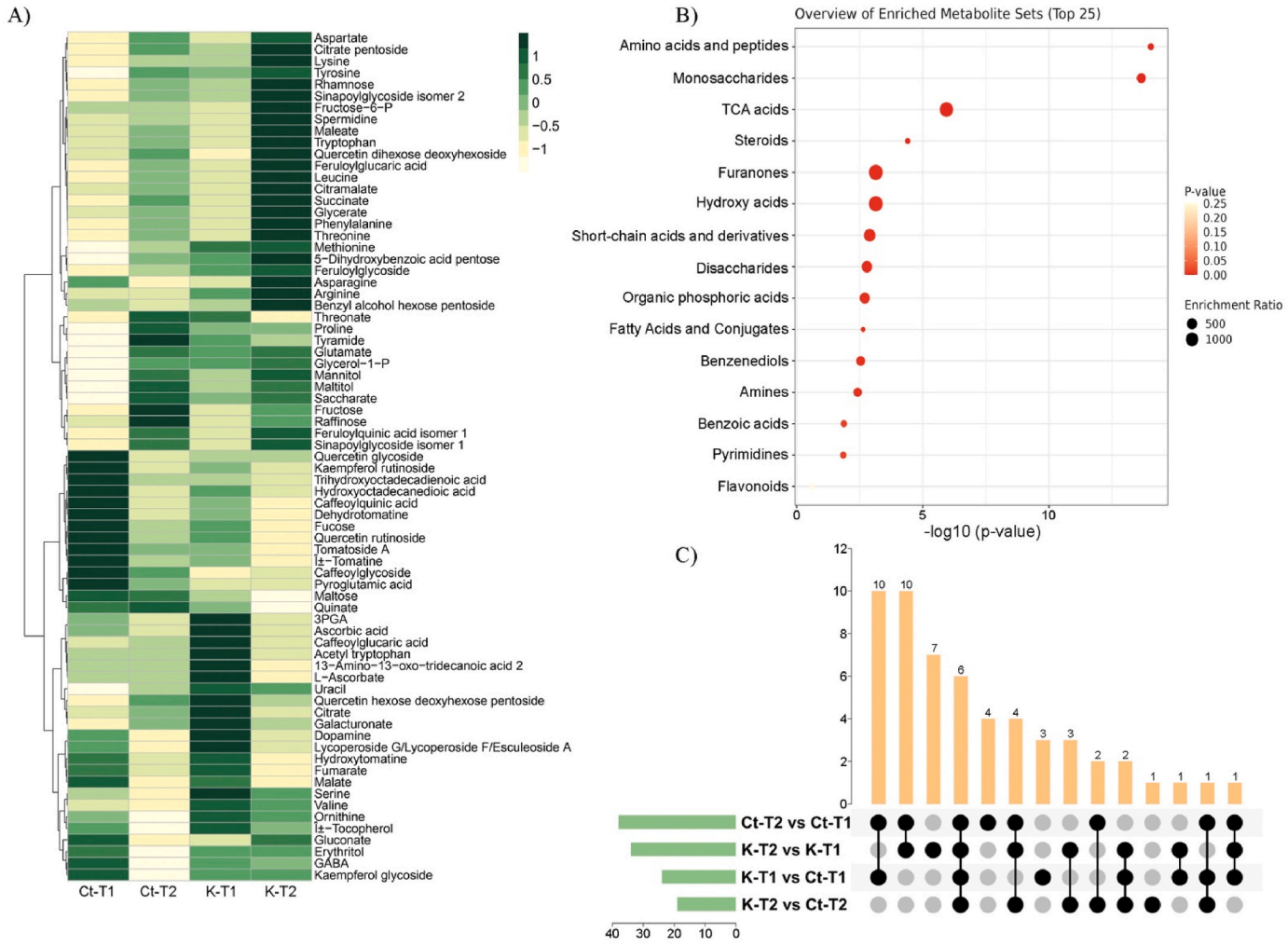

Fig. 4. Metabolomic comparison of leaves from *K. rhizophila*-inoculated (K) and non-inoculated (Ct) tomato plants. **A)** Heatmap of scaled metabolite amounts recorded for each treatment at different times (T1 and T2). **B)** Enriched metabolite analysis. The data for each class are reported in Table S7. **C)** UpSet Venn diagram of differentially accumulated metabolites (DAMs) deriving from different treatments and times (Ct-T2 vs. Ct-T1; K-T2 vs. K-T1; K-T1 vs. Ct-T1; K-T2 vs. Ct-T2). The horizontal bar chart on the left shows the element (count of differential metabolites; up numbers indicate the elements for each comparison) statistics for each comparison group. A single black dot represents a grouping specific element, and the lines between points represent the intersection specific to different groupings. The vertical bar chart represents the number of corresponding intersection elements.

caused a differential accumulation of some proteins involved in signaling pathways related to important biological mechanisms. For example, protein ubiquitination-related ubiquitin carboxyl-terminal hydrolase (UCH; Solyc07g063650.3) and UBX domain-containing protein (Solyc08g080410.3.1) were down-represented in K samples, while glycolytic enzymes - protein related to reactive oxygen species (ROS) - and growth-controlling nucleoside diphosphate kinase (Solyc03g110960.3) were over-represented therein.

3.5. Metabolite variance and pathway analysis in *K. rhizophila*-treated plants

To investigate metabolite variations in tomato due to *K. rhizophila* treatment, the metabolome of K and Ct leaves, at each sampling time, was developed by HPLC/MS. Seventy-three metabolites were detected, with significant differences in their amount between treatments and times (Fig. 4A). At T1, quantitative levels of some compounds related to tricarboxylic acid (TCA) cycle were significantly higher in K than Ct samples; a similar phenomenon was observed for some amino acids (*e.g.*, valine, serine, methionine, tyrosine, ornithine), dopamine, various carbohydrates, and some antioxidant substances (*e.g.*, L-ascorbate)

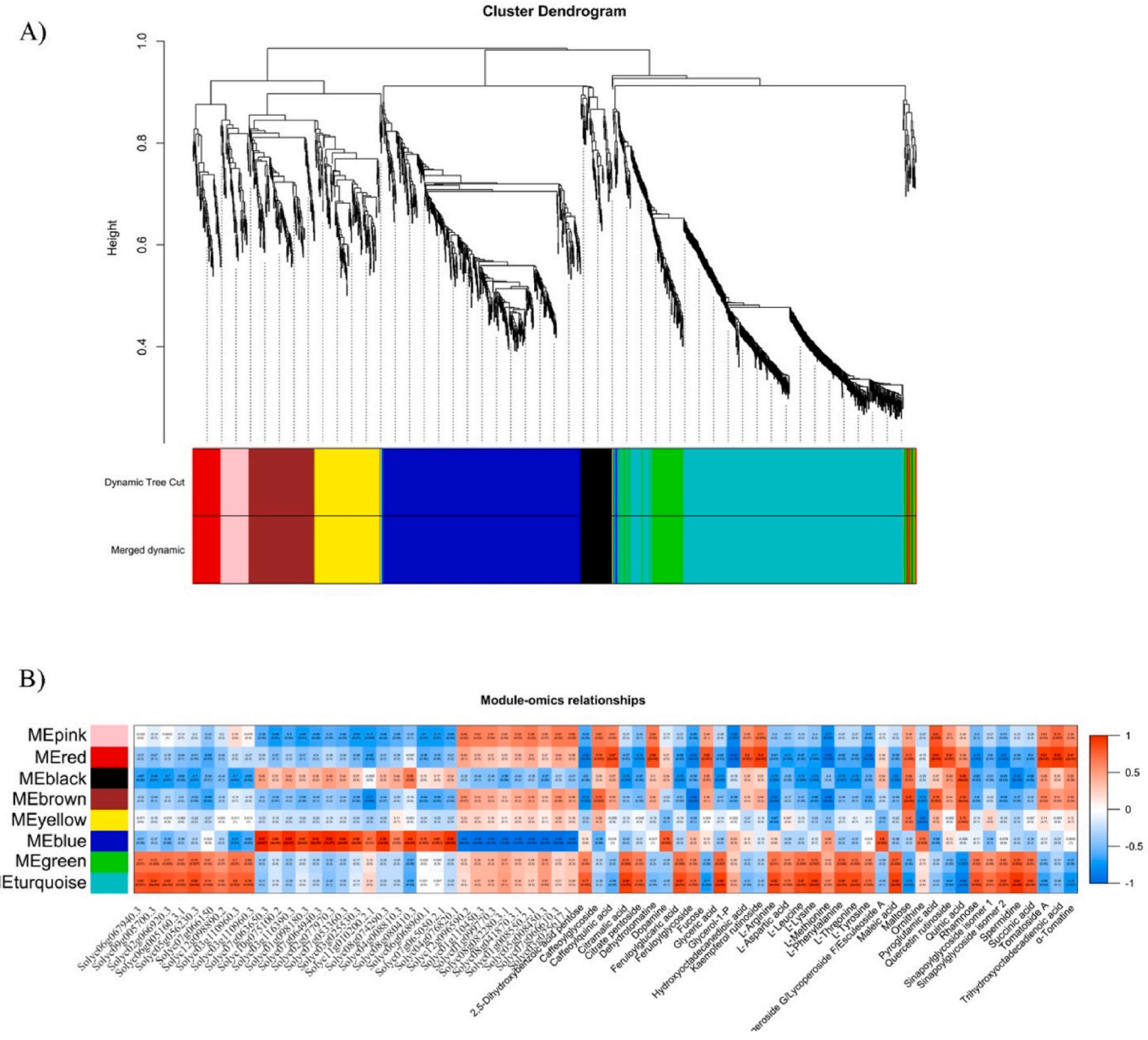

Fig. 5. Weighted gene co-expression network analysis (WGCNA) of leaf genes modulated by the application of *K. rhizophila* to tomato plants. **A)** Establishment of a Gene clustering tree (dendrogram) obtained via hierarchical clustering of topological overlapping dissimilarity. Dendrogram showing the co-expression modules identified by WGCNA across time in the *K. rhizophila*-treated plants. The major tree branches constitute eight modules labeled with different colors (see also Table S9). **B)** Correlation heatmap among genes belonging to the eight most significant modules extracted (having the same coloring of that shown in panel A), and the other factors (proteins and metabolites) investigated in this study. Each row corresponds to a module, and each column represents a specific compound (protein or metabolite) as resulting from proteomic and metabolomic analysis. The color of each cell at the row-column intersection indicates the Pearson's correlation coefficient (*p-value* was indicated in bracket) between module and trait. Red indicates the positive correlation between module and trait, while blue shows the negative correlation.

(Fig. 4A). At T2, a similar trend between treatments (K *vs*. Ct) was observed. Indeed, above-mentioned amino acids as well as asparagine, lysine, tryptophan, leucine, and others were significantly increased in K compared to Ct samples. Conversely, the concentration of fructose and raffinose and other sugars selectively decreased in K samples. Focusing on other carbohydrates, such as mannitol, maltitol, and saccharate, their amount showed a common quantitative trend for K and Ct plants at T2 (Fig. 4A), showing in both cases higher levels at T2 compared to that measured at T1. Finally, proline showed a mixed behavior; at T1, it evidenced a slight accumulation in K samples compared to Ct ones, which was followed at T2 by a significant increase in Ct, while corresponding K levels remained constant.

When metabolomic data were subjected to enrichment analysis, 15 classes were identified, in which "amino acids and peptides", "monosaccharides", and "TCA" were the most significant ones (Fig. 4B; Table S7). Among that, significant Differentially Accumulated Metabolites (DAMs) were observed in pairwise comparisons (Fig. 4A and C). By comparing DAMs of K and Ct at the same sampling time (K-T1 *vs*. Ct-T1 and K-T2 *vs*. Ct-T2), this analysis highlighted 3 (caffeoylglycoside, feruloylglycoside, and uracil) and 1 (maltose) unique DAMs at T1 and T2, respectively, which were induced by *K. rhizophila* treatment (Fig. 4C; Table S8). By comparing DAMs within K and Ct groups over different sampling times (K-T2 *vs*. K-T1 and Ct-T2 *vs*. Ct-T1), 7 and 4 unique DAMs were revealed in K and Ct plants, respectively (Fig. 4C; Table S8). The most impact pathways extracted were "alanine, aspartate and glutamate metabolism", with an accumulation of aspartate and succinate, as well as "isoquinoline alkaloid biosynthesis", showing a greater amount of tyrosine and dopamine, depending on *K. rhizophila* treatment (Table S9).

3.6. Weighted gene co-expression network analysis of multi-omics data

Based on identified DEGs, DAPs and DAMs, a co-expression network analysis through the Weighted Gene Co-expression Network Analysis (WGCNA) tool was carried out to identify the most relevant modules and relative pathways associated to *K. rhizophila* treatment in tomato. Eight modules were isolated through a hierarchical linkage clustering, and 3 out of 8 modules were strongly correlated to several variables (Fig. 5A and B). The "turquoise" module showed the highest correlation coefficient ($r > 0.80$; $P < 0.01$), followed by the "green" one ($r > 0.70$, $P < 0.01$). These two modules exhibited a comparable correlation between genes and the same set of proteins, such as UBX domain-containing protein (Solyc08g080410.3.1), nucleoside diphosphate kinase (Solyc03g110960.3), cytosolic ascorbate peroxidase 1 (Solyc06g005160.3.1), a putative structural component of ribosome (Solyc12g098890.2), and various metabolites, which included some amino acids and TCA compounds, and dopamine (Fig. 5B). By contrast, the "blue" module was strongly correlated with proteins mainly accumulated at T1 in *K. rhizophila*-treated samples ($r > 0.80$, $P < 0.01$), showing a negative correlation ($r > -0.90$, $P < 0.01$) to other proteins (Fig. 5B). In the same module, only 3 out of 37 metabolites (dopamine, lycoperoside, and ornithine) showed high positive and significant correlation ($r > 0.72$, $P < 0.01$) (Fig. 5B).

To explore the biological relevance of genes and pathways included in the three main identified modules (turquoise, green, and blue), a GO enrichment analysis was performed. The "turquoise" module consisted of 575 genes, whose functions were mainly included in the BP category "response to biotic stimulus" (GO: 0009607), the MF category "protein binding" (GO: 0005515), and the CC category "cell periphery" (GO: 0071,944) (Table S10). In this module, genes coding a cytochrome P450 isoform (Solyc02g070580.1.1) and AOS (Solyc04g079730.1.1) were included, together with six hub genes with higher connectivity, coding kinesin family member C1 (Solyc11g071730.3.1), ribosomal RNA-processing protein 7 (RRP7) (Solyc02g089600.3.1), translation initiation factor eIF4E (Solyc03g005870.4.1), β-galactosidase (Solyc04g080840.3.1), tzinc finger protein CONSTANS 1 (CO1) (Solyc02g089540.3.1), and peroxisomal membrane protein Pex16 (Solyc01g091900.3.1) (Table S10; Fig. S8). One hundred and two genes belonging to the "green" module were included in "root hair cell differentiation" (BP, GO: 0048,765), "trichoblast maturation" (BP, GO: 0048,764), "cellular response to chemical stimulus" (BP, GO: 0070,887), and "membranes" (CC, GO: 0016,020) categories. Six hub genes coding a Ser/Thr-protein kinase (Solyc12g005290.2.1), a purine nucleobase transmembrane transport protein (PUNUT) (Solyc08g077370.4.1), a ferredoxin [2Fe–2S] (Solyc08g077050.3.1), a SIG5 14-3-3 family protein (Solyc04g012120.3.1), a multi antimicrobial extrusion component (MATE) (Solyc03g026230.1.1), and a subtilase family member (Solyc01g087840.3.1) were identified in the green module (Table S10; Fig. S8). Finally, the "blue" module comprised 457 genes, many of which correlated to important biological processes, such as those associated with "metal ion homeostasis" (GO:0055,065), "potassium ion transmembrane transport" (GO:0071,805), "response to karrikin" (GO:0080,167; a class of germination stimulants), "post-embryonic development" (GO:0009791), "stomatal complex patterning" (GO:0010,374) categories (Table S10; Fig. S8). Here, genes coding SAMDC (Solyc06g054460.1.1) and a plasmodesmal protein (Solyc09g090680.3.1) were observed, as well as six hub genes with a high degree of connectivity, coding a hydroxyphenylpyruvate reductase (HPPR) (Solyc12g044250.2.1), a KDEL-tailed cysteine endopeptidase (CysEP) (Solyc03g111730.3.1), a zinc-finger component (E3 ubiquitin protein ligase) (Solyc03g032060.1.1), a BRO1-like domain component (BRO1) (Solyc03g019950.3.1), a PI-3-kinase-related kinase (SMG-1) (Solyc01g109080.3.1), and a peptide-methionine (R)-S-oxide reductase/selenoprotein R (SelR) (Solyc01g080410.3.1) (Table S10; Fig. S8).

4. Discussion

Plant Biostimulants (PBs) are products exerting beneficial effects on plants through the improvement of the nutrients use efficiency, the implementation of fruit quality, and tolerance to abiotic stress (EU, 2019; https://eur-lex.europa.eu/). Their positive effects have been already demonstrated on tomato yield and fruit quality, as well as their growth-promoting and stress-ameliorating effects under salt stress (Colla et al., 2017). However, the action mode of PBs is still largely unknown. Here, key molecular players activated by *K. rhizophila* treatment in tomato have been identified through a multi-omics approach, highlighting their role in plant growth and development.

4.1. DEGs enrichment analysis reveals impacted plant molecular pathways after K. rhizophila application

K. rhizophila treatment determined evident transcriptomic changes in tomato leaves at both T1 and T2, compared to control, which unveiled specific molecular pathways elicited by this PGPB. As expected, a significant number of DEGs were identified in all pairwise comparisons, with the highest number of them observed when comparing K and Ct plants at T2 (K-T2 *vs*. Ct-T2). In general, *K. rhizophila* application was able to trigger transcriptional changes of various gene typologies; a GO enrichment analysis of DEGs evidenced a significant over-expression of genes involved in the "cellular response to stimulus", "cellular response to stress", "macromolecule catabolic process", "polysaccharide catabolic process", "intercellular transport", "plasmodesmata-mediated intercellular transport", and "steroid and sterol metabolic processes" categories. In particular, *K. rhizophila* treatment increased the expression of genes coding plasmodesmal proteins (PDs) (Solyc03G005690.3.1 and Solyc06G083750.3.1), a class of cytoplasmic membrane-lined channel components involved in the molecules transport across plant cells (Burch-Smith et al., 2011). Interestingly, PDs mediated the brassinosteroids (BRs) transport among cells, a class of steroidal plant hormones involved in the regulation of plant growth and development (Ali, 2019). In agreement with this observation, the GO category "steroid and sterol metabolic process" resulted positively enriched after *K. rhizophila* treatment and included a gene coding a cytochrome P450 enzyme

(Solyc02g070580.1.1) involved in BRs biosynthesis (Enoki et al., 2023). A *K. rhizophila*-dependent enrichment was also observed for two genes coding allene oxide synthases (AOS. Solyc04g079730.1.1; Solyc11g069800.1.1) involved jasmonic acid (JA) biosynthesis. Interestingly, JA is a plant growth regulator whose cross-talking with other hormones regulates plant growing and defense response (Yang et al., 2019).

Furthermore, *SAMDC* (Solyc06g054460.1.1), included in the "amine metabolic process", was up-regulated after *K. rhizophila* treatment. *SAMDC* seems to play an important role in plant growth and development, also under stress conditions; indeed, high levels of *SAMDC* enhanced vegetative growth and induced an early flowering in tobacco (Zhu et al., 2020a), while its over-expression improved cold tolerance in maize and turfgrass (Luo et al., 2017; Jiao et al., 2022). SAMDC is able to decarboxylate S-adenosylmethionine (SAM) favoring spermidine or spermine production; alternatively, SAM can be converted into 1-aminocyclopropane 1-carboxylic acid (ACC), a precursor of ethylene, a key plant growth hormone. *SAMDC* expression levels are driven by several metabolites, including dopamine, a catecholamine neurotransmitter which has been here demonstrated having higher levels in K than Ct samples at T1 and T2. Recently, dopamine has been reported to play a key role in mediating plant growth by increasing the carbon and nitrogen metabolism, and levels of the corresponding enzymes (Lan et al., 2020). Finally, a gene coding an inositol transporter (Solyc12g099070.1.1) belonging to "inorganic anion transport", was up-regulated after *K. rhizophila* treatment. These proteins are already known to transport several metabolites, such as lipids, minerals, and sugars, and play an important role in plant signaling pathways regulating message transduction processes also involving hormones, neurotransmitters, and growth factors (Zhou et al., 2022).

Among *K. rhizophila*-dependent down-regulated genes, worth mentioning are specific transcripts belonging to the "small molecule biosynthesis processes" category, which are involved in photosynthesis, electron transport chain, light harvesting complex, and tetrapyrrole pathway. The observed down-regulation of genes involved in photosynthesis and electron transport chain could lead a ROS accumulation in cell organelles, that justified the concomitant up-regulation in *K. rhizophila*-treated plants of genes involved in the "cellular response to stress" category, such as those coding mitogen-activated protein kinases (*MAPKs*; Solyc02g090990.1.1; Solyc08g076490.2.1) and heat stress transcription factors (*HSF*; Solyc02g079180.1.1). The important role of *MAPKs* and *HSFs* in the transduction of environmental and developmental signals through the phosphorylation of downstream targets, also included in ROS balancing, was already reported (Hoang et al., 2019). Although the enrichment of *K. rhizophila*-dependent DEGs related to photosynthesis and light harvesting complex may suggest a possible discrepancy with the corresponding proteomic results (see the dedicated paragraphs), the evidences can be explained by the possible fulfillment of proteins translation process of the genes belonging to these categories at the sampling times. In addition, the occurrence of additional post-transcriptional processes can also be eventually considered for specific components. All together, these results proved a significant reorganization of various photosynthetic machineries as result of *K. rhizophila*-tomato plant interaction.

A number of other genes involved in plant defense were down-regulated after *K. rhizophila* challenge, in agreement with similar evidences on other PGPB. Recently, transcriptomic analysis focused on plant-*Herbaspirillum seropedicae* interaction in rice showed the down-regulation of genes coding pathogenesis-related proteins (PRPs), chitinases, thionins, and cinnamoyl-CoA-reductases, which are all well-known components involved in disease resistance mechanisms (Wiggins et al., 2022). Thus, the present study further supports the idea that, after its interaction with beneficial microbes, the host plant adjusts its transcriptomic profile to regulate molecular mechanisms potentially preserving organism health.

Our general findings on a significant deregulation of gene expression after *K. rhizophila* treatment were independently supported by the overall methylation levels measured in PGPB-challenged plants. DNA methylation is a major epigenetic modification driving the expression of genes associated to key biological mechanisms, including plant growth and development (Zhang et al., 2018). The methylation status of DNA in plant is easily affected by physiological factors, developmental stages, and environment, and its changes cause the difference of gene expression levels. Therefore, the significant higher DNA methylation triggered by *K. rhizophila* treatment agreed with the modified transcriptomic profiles here observed.

4.2. DAPs enrichment analysis reveals impacted plant pathways after K. rhizophila application

Quantitative proteomic experiments revealed various DAPs associated with *K. rhizophila* treatment, involved in energy (photosystem) and nutrient (carbohydrate and amino acids) metabolism. In particular, an over-representation of several proteins playing a key role in photosynthesis, namely photosystem I (subunit IV and V, also named PSI-G) and II (various Psb family proteins) reaction center components, as well as photosynthetic NDH subcomplex protein, thylakoid membrane phosphoprotein, chlorophyll *a-b* binding protein, and ATP synthase delta-subunit protein, was observed. In accordance with previous results in other plants, Psb family proteins are essential components highly affecting plant growth rate (Hackett et al., 2017), while PSI-G protein is over-represented in plants whose salt and drought tolerance is increased by a mutualistic interaction with the root microbiome (Roy et al., 2021). Moreover, the over-representation of various photosystem I and II components, including PSI-G, was already described in barley interacting with fungal endophytes (Ghaffari et al., 2019). Together with transcriptomic results, these observations proved a significant reorganization of the tomato leaf photosynthetic machineries after *K. rhizophila* interaction to afford an optimized photosynthetic capacity for coping plant growth and development.

Furthermore, *K. rhizophila* treatment on tomato induced the over-representation of proteins related to abiotic stress response, such as the cytosolic ascorbate peroxidase 1 (APX1), which is able to mitigate the effects of oxidative bursts, playing a key role in H_2O_2 removal and regulation of ROS impact (Davletova et al., 2005). In the latter context, nucleoside diphosphate kinase involved in the synthesis of nucleoside triphosphates other than ATP was found over-represented in *Kocuria*--treated plants. Plants over-expressing the latter kinase were already described being tolerant to paraquat pesticide as result of their improved ability to remove H_2O_2 (Sandalio et al., 2013). Other key proteins were over-represented in tomato leaves after *K. rhizophila* treatment, such as the ubiquitin carboxyl-terminal hydrolase (UCH), which participates in key cellular processes including signal transduction and transcription. Through their deubiquitylation activity, the UCH members family regulated the auxin/indole-3-acetic acid ratio, which influences auxin-dependent developmental pathways in *Arabidopsis* (Hayama et al., 2019). Moreover, the observed over-representation of different phosphofructokinases in K plants was in perfect agreement with their role in sugar metabolism, cell expansion and plant growth (Beauvoit et al., 2014). All together, these proteomic results unveiled key molecular mechanisms induced after *K. rhizophila* treatment, providing a rationale for the fortifying the PGPB role in promoting plant growth and development as well as in mitigating possible abiotic stresses.

4.3. Metabolites profiling changes and DAMs in tomato by K. rhizophila application

Significant metabolomic changes were observed in *K. rhizophila* inoculated plants. Interestingly, the most represented DAMs resulting from treated plants belonged to amino acids and carbohydrates. Pathways related to "alanine, aspartate and glutamate" metabolism as well as to "isoquinoline alkaloid biosynthesis" were significantly affected by

the PGPB treatment at both sampling times. A significant change of "alanine, aspartate and glutamate" metabolism was already described to be associated with an enhancement of abiotic stress tolerance (Abd El-Daim et al., 2020), while that of "isoquinoline alkaloid biosynthesis" was previously reported to remove ROS, mitigating the oxidative stress in plant cells (Gong et al., 2020).

The present study originally evidenced high levels of dopamine in K *vs.* Ct samples at both sampling times. Dopamine was recently proved as a plant metabolite having a specific regulative role in redox stress response (Raza et al., 2022) as well as in plant growth and development, stimulation of photosynthesis and plant immune response (Liu et al., 2020). Indeed, endogenous dopamine levels affected the expression of many genes related to abiotic stresses, such as drought, salt and nutrient ones, or affecting plant growth through an increased carbon and nitrogen metabolism (Lan et al., 2020). Among that, worth mentioning is *SAMDC*, which was up-regulated in *K. rhizophila* inoculated plants, confirming the positive correlation between transcriptomic and metabolomic results, and highlighting the multi-regulatory role of dopamine in coordinating several physiological events (Raza et al., 2022).

Among over-represented DAMs in K treated plants, worth mentioning are feruloyl glycoside and other glycosylated phenolic compounds having antioxidant and anti-inflammatory properties. The accumulation of feruloyl glycoside has been recently associated with the progression of plant growth cycle in cactus *Turbinicarpus* (Solis-Castañeda et al., 2020).

In conclusion, the metabolomic profiles of *K. rhizophila*-treated plants agreed to and integrated the findings provided by transcriptomic and proteomic findings, further underlining that the PGPB studied modulates carbon sources and energy in the host, and affects the levels of various messengers, like dopamine, regulating the expression of genes involved in plant growth and development as well as in response to abiotic stresses.

4.4. Integration of multi-omics data from K. rhizophila-inoculated plants

Plant response to PGPBs is associated with a complex network of linked pathways driving specific responses of genes, proteins and metabolites, which are involved in important biological processes. By using a WGCNA approach, we here identified eight gene modules regulating tomato response to *K. rhizophila* treatment, based on their significant correlation with variably accumulated proteins and metabolites (DAPs and DAMs). According to their relation, both the turquoise and green modules showed the highest correlation with nine proteins, including above-discussed nucleoside diphosphate kinase involved in energy homeostasis and plant developmental processes (Ye et al., 2020), cytosolic ascorbate peroxidase 1 associated with response to abiotic stress (X. Li et al., 2020), and several metabolites mostly related to amino acid metabolism and TCA cycle.

In the turquoise module, six hub genes were identified as deregulated after *K. rhizophila* treatment, which code kinesin family member C1, ribosomal RNA-processing protein 7 (RRP7), translation initiation factor eIF4E, β-galactosidase, zinc finger protein CONSTANS 1 (CO1) (Solyc02g089540.3.1), and peroxisomal membrane protein Pex16. Kinesins are motor proteins able to regulate gibberellin biosynthesis and cell growth through transcriptional activity (Nebenführ and Dixit, 2018); they also affect microtubule organization, organelle distribution and vesicle transport. Overall, kinesins contribute directly and indirectly to cell division and growth in several plant tissues (Nebenführ and Dixit, 2018). RRP7 is a ribosome biogenesis factor required for 18S ribosomal RNA (rRNA) maturation. Interestingly, a *rrp7* mutant in *Arabidopsis* showed slow growth, altered shoot phyllotaxy, and abscisic acid hypersensitivity (Micol-Ponce et al., 2018). The eIF4E regulation under abiotic stress conditions was already reported as a molecular mechanism involved in the recognition of mRNA cap, ATP-dependent unwinding of 5′-terminal secondary structures and mRNA recruitment to the ribosome (Zhu et al., 2020b). Furthermore, β-galactosidase plays key roles in the modification of cell wall components in several physiological processes, including fruit ripening, flower senescence and cell wall loosening during plant growth (Ahn et al., 2007). CO1 transcription factor has already been described to regulate a series of cellular processes in plants, including the transition from the vegetative growth to flower development; its role in regulating plant growth and fruit yield in tomato is poorly understood (Cui et al., 2022). Finally, Pex16 seems responsible for importing peroxisomal membrane proteins whose targeting signal has not yet well-defined (Akther et al., 2022). A *pex16* mutant in *Arabidopsis* appeared defective in the peroxisomes formation and the transport of plasma membrane- and cell wall-associated proteins, suggesting a role of this component in seed protein storage (Lin et al., 1999). Among the other genes included in the turquoise module, worth mentioning are those coding cytochrome P450 isoform and AOS, which are involved in the BRs and JA biosynthesis, respectively (Enoki et al., 2023; Yang et al., 2019).

In the green module, six hub genes were identified as deregulated after *K. rhizophila* treatment, which code a Ser/Thr-protein kinase, a purine nucleobase transmembrane transport protein (PUNUT), a ferredoxin [2Fe–2S], a SIG5 14-3-3 family protein, a multi-antimicrobial extrusion component (MATE) and a subtilase family member. By introducing post-translational modifications affecting structure and activity of target proteins, Ser/Thr-protein kinases play a significant role in many cellular processes, including regulation of cell proliferation/differentiation and embryonic development. Interestingly, they are involved in various abiotic stress responses as well as in abscisic acid response, calcium signaling and antioxidant defense (Ye et al., 2017). Ferredoxins [2Fe–2S] play an important role in electron transfer processes and various enzymatic reactions associated with photosynthesis; they are also involved in the redox stress regulation, cell proliferation and N fixation processes (Nechushtai et al., 2020). SIG-5 14-3-3 protein belongs to a ubiquitous family of pSer/pThr-binding proteins, which play important roles in many biological processes modulated by phosphorylation, including cell cycle regulation, protein trafficking, plant growth and development, cell elongation and division. The MATE transporters are involved in plant growth and stress responses (Ku et al., 2022); interestingly, allelic forms and expression patterns of MATE have been reported to be associated with favorable agronomic traits in domesticated crops. Finally, subtilases are involved in the plant life cycle, regulating development of seeds and fruits, cell wall modification, processing of peptide growth factors and epidermal development; they were also associated with plant response to biotic and abiotic stresses (Figueiredo et al., 2018).

In the blue module, six hub genes with a high degree of connectivity with the other joining genes, code a hydroxyphenylpyruvate reductase (HPPR), KDEL-tailed cysteine endopeptidase (CysEP), a zinc-finger (E3 ubiquitin protein ligase), a BRO1-like domain (BRO1), a PI-3-kinase-related kinase (SMG-1) and a peptide-methionine (R)-S-oxide reductase/selenoprotein R (SelR). Interestingly, all the above-reported hub genes appear involved in plant growth and development as well as in abiotic stresses adaptation. Indeed, HPPR is the key enzyme assisting the conversion of tyrosine to 4-hydroxyphenyl-lactic acid (pHPL); this metabolite was already reported having different functions in plant growth, development, and adaptation (Xu et al., 2018). Similarly, *CysEP* plays a role in regulating plant growth and development (Wen et al., 2021) and high resilience tomato plants to abiotic stresses showed a high expression of this gene. The E3 ubiquitin protein ligase is a multifunctional enzyme that plays important roles during various plant growth stages, affecting several abiotic stress responses (Shu and Yang, 2017). BRO1 is a constituent of the endosomal sorting complex required for transport (ESCRT) machinery that controls the homeostasis of membrane proteins by selective vacuolar degradation (Shen et al., 2018); it is a determinant for multiple physiological functions during cell growth and differentiation. On the other hand, SMG-1 regulates several eukaryotic cellular processes including cell-signaling cascades related to

DNA damage and repair, as well as cell growth and proliferation (Angira et al., 2020). *SelR* gene encodes a peptide methionine sulfoxide reductase mediating reduction of oxidized methionine, an important reaction by which cells regulate biological processes and cope with oxidative stress. *SelR* overexpression was already associated with an increase of plant protection against abiotic and biotic environmental constraints (Rey and Tarrago, 2018). Finally, *SAMDC* and the Solyc09g090680.3.1 gene coding a plasmodesmal protein were also grouped in the blue module; the first gene and the protein coded from the second one seem modulated by dopamine and BRs, respectively (Wang et al., 2023). The first metabolite strongly correlated to this module. The linkage between genes/proteins modulated by these metabolites, dopamine and BRs has already been emphasized in recent studies on hormone regulators involved in plant growth and development as well as in response to abiotic stresses (Liu et al., 2020; Raza et al., 2022).

5. Conclusion

In this study the molecular mechanisms associated with the PGP action of *K. rhizophila* on tomato plants have been highlighted through a multi-omics approach allowing us to identify some key hub genes and metabolic pathways activated after PGPB treatment. Although further studies are required to obtain functional details on the plant molecular mechanisms affected by *K. rhizophila* treatment, this work sheds light on its putative role in the modulation of specific cellular processes, giving a possible explanation for the improved growth and development by an enhanced nutritional and metabolic capability. A complex machinery including selected genes, proteins, and specific plant metabolites, including sugars, amino acids, energy regulators, and other factors such as dopamine is strongly modulated by the PGPB-plant interaction contributing to the implemented plant growth. On this basis, these selected components can be considered key factors necessary for improving plant yield in dedicated PGPB-mediated agriculture strategies.

Funding

This research was funded by BIAS - Innovative biofertilizers for sustainable agriculture to protect human health and the environment (project number 082015000275), funded by Sicily Region through the European Regional Development Fund (PO-FESR Sicilia, 2014–2020). The research was also partially funded by the Agritech National Research Center funded within the European Union NextGeneration EU program (the National Recovery and Resilience Plan, mission 4, component 2, investment 1.4 – D.D. 1032 del June 17, 2022, project CN00000022). This manuscript reflects only the authors' views and opinions, neither the European Union nor European Commission can be considered responsible for them.

CRediT authorship contribution statement

Antonio Mauceri: Writing – review & editing, Writing – original draft, Investigation, Formal analysis. **Guglielmo Puccio:** Writing – review & editing, Writing – original draft, Validation, Investigation, Formal analysis, Data curation. **Teresa Faddetta:** Writing – review & editing, Investigation, Formal analysis, Data curation. **Loredana Abbate:** Writing – review & editing, Investigation. **Giulia Polito:** Writing – review & editing, Formal analysis. **Ciro Caldiero:** Writing – review & editing, Investigation. **Giovanni Renzone:** Writing – review & editing, Validation, Investigation, Formal analysis. **Margot Lo Pinto:** Writing – review & editing, Investigation. **Pasquale Alibrandi:** Writing – review & editing, Formal analysis. **Edoardo Vaccaro:** Writing – review & editing, Investigation. **Maria Rosa Abenavoli:** Conceptualization, Writing – review & editing. **Andrea Scaloni:** Conceptualization, Writing – review & editing. **Francesco Sunseri:** Conceptualization, Writing – review & editing. **Vincenzo Cavalieri:** Formal analysis, Investigation, Writing – review & editing. **Antonio Palumbo Piccionello:** Formal analysis, Investigation, Writing – review & editing. **Giuseppe Gallo:** Conceptualization, Formal analysis, Funding acquisition, Investigation, Writing – review & editing. **Francesco Mercati:** Conceptualization, Formal analysis, Funding acquisition, Supervision, Validation, Writing – original draft, Writing – review & editing.

Declaration of competing interest

The authors declare that they have no known competing financial interests or personal relationships that could have appeared to influence the work reported in this paper.

Data availability

The data presented in this study are available in the text or downloading by links included in the manuscript or in Supplementary material here

Acknowledgements

We thank the H2020 Europe Project: PRO-GRACE - Promoting a Plant Genetic Resource Community for Europe (grant agreement ID: 101094738) for providing information and network.

Appendix A. Supplementary data

Supplementary data to this article can be found online at https://doi.org/10.1016/j.plaphy.2024.108609.

References

Abd El-Daim, I.A., Bejai, S., Meijer, J., 2020. *Bacillus velezensis* 5113 induced metabolic and molecular reprogramming during abiotic stress tolerance in wheat. Sci. Rep. 9, 16282.

Ahn, Y.O., Zheng, M., Bevan, D.R., Esen, A., Shiu, S.H., Benson, J., Peng, H.P., Miller, J. T., Cheng, C.L., Poulton, J.E., Shih, M.C., 2007. Functional genomic analysis of *Arabidopsis thaliana* glycoside hydrolase family 35. Phytochem 68, 1510–1520.

Ali, B., 2019. Brassinosteroids: the promising plant growth regulators in horticulture. In: Hayat, S., Yusuf, M., Bhardwaj, R., Bajguz, A. (Eds.), Brassinosteroids: Plant Growth and Development, vol. 1, pp. 349–365. Spr.

Angira, D., Shaik, A., Thiruvenkatam, V., 2020. Structural and strategic landscape of PIKK protein family and their inhibitors: an overview. Front. Biosci. 25, 1538–1567.

Bartucca, M.L., Cerri, M., Del Buono, D., Forni, C., 2022. Use of biostimulants as a new approach for the improvement of phytoremediation performance-A review. Plants 11, 1946.

Beauvoit, B.P., Colombié, S., Monier, A., Andrieu, M.H., Biais, B., Bénard, C., Chéniclet, C., Dieuaide-Noubhani, M., Nazaret, C., Mazat, J.P., Gibon, Y., 2014. Model-assisted analysis of sugar metabolism throughout tomato fruit development reveals enzyme and carrier properties in relation to vacuole expansion. Plant Cell 26, 3224–3242.

Burch-Smith, T.M., Brunkard, J.O., Choi, Y.G., Zambryski, P.C., 2011. Organelle–nucleus cross-talk regulates plant intercellular communication via plasmodesmata. Proc. Natl. Acad. Sci. U.S.A. 108, 1451–1460.

Cao, S., Guo, M., Wang, C., Wu, W., Shi, T., Tong, G., Zheng, C., Cheng, H., Elcheeri, N.I., Cheng, Y., 2019. Genome-wide characterization of aspartic protease (AP) gene family in *Populus trichocarpa* and identification of the potential PtAPs involved in wood formation. BMC Plant Biol. 19, 276.

Colla, G., Cardarelli, M., Bonini, P., Rouphael, Y., 2017. Foliar applications of protein hydrolysate, plant and seaweed extracts increase yield but differentially modulate fruit quality of greenhouse tomato. Hortic. Sci. (Stuttg.) 52, 1214–1220.

Cui, L., Zheng, F., Wang, J., Zhang, C., Zhang, D., Gao, S., Zhang, C., Ye, J., Zhang, Y., Ouyang, B., Wang, T., Hong, Z., Ye, Z., Zhang, J., 2022. The tomato CONSTANS-LIKE protein SlCOL1 regulates fruit yield by repressing SFT gene expression. BMC Plant Biol. 22, 429.

Davletova, S., Rizhsky, L., Liang, H., Shengqiang, Z., Oliver, D.J., Coutu, J., Shulaev, V., Schlauch, K., Mittler, R., 2005. Cytosolic ascorbate peroxidase 1 is a central component of the reactive oxygen gene network of *Arabidopsis*. Plant Cell 17, 268–281.

De Andrade, L.A., Santos, C.H.B., Frezarin, E.T., Sales, L.R., Rigobelo, E.C., 2023. Plant growth-promoting rhizobacteria for sustainable agricultural production. Microrganisms 11, 1088.

Del Giudice, R., Petruk, G., Raiola, A., Barone, A., Monti, D.M., Rigano, M.M., 2017. Carotenoids in fresh and processed tomato (*Solanum lycopersicum*) fruits protect cells from oxidative stress injury. J. Sci. Food Agric. 97 (5), 1616–1623.

Drobek Abd El-Daim, I.A., Bejai, S., Meijer, J., 2019. *Bacillus velezensis* 5113 induced metabolic and molecular reprogramming during abiotic stress tolerance in wheat. Sci. Rep. 8 (1), 16282, 9.
Du Jardin, P., 2015. Plant biostimulants: definition, concept, main categories and regulation. Sci. Hortic. 196, 3–14.
Enoki, S., Tanaka, K., Moriyama, A., Hanya, N., Mikami, N., Suzuki, S., 2023. Grape cytochrome P450 CYP90D1 regulates brassinosteroid biosynthesis and increases vegetative growth. Plant Physiol. Biochem. 196, 993–1001.
Faddetta, T., Abbate, L., Renzone, G., Palumbo Piccionello, A., Maggio, A., Oddo, E., Scaloni, A., Puglia, A.M., Gallo, G., Carimi, F., Fatta del Bosco, S., Mercati, F., 2018. An integrated proteomic and metabolomic study to evaluate the effect of nucleus-cytoplasm interaction in a diploid citrus cybrid between sweet orange and lemon. Plant Mol. Biol. 98, 407–425.
Faddetta, T., Polito, G., Abbate, L., Alibrandi, P., Zerbo, M., Caldiero, C., Reina, C., Puccio, G., Vaccaro, E., Abenavoli, M.R., Cavalieri, V., Mercati, F., Palumbo Piccionello, A., Gallo, G., 2023. Bioactive metabolite survey of actinobacteria showing plant growth promoting traits to develop novel biofertilizers. Metabolites 13, 374.
Figueiredo, J., Sousa, S.M., Figueiredo, A., 2018. Subtilisin-like proteases in plant defence: the past, the present and beyond. Mol. Plant Pathol. 19 (4), 1017–1028.
Ghaffari, M.R., Mirzaei, M., Ghabooli, M., Khatabi, B., Wu, Y., Zabet-Moghaddam, M., Mohammadi-Nejad, G., Haynes, P.A., Hajirezaei, M.R., Sepehri, M., Salekdeh, G.H., 2019. Root endophytic fungus *Piriformospora indica* improves drought stress adaptation in barley by metabolic and proteomic reprogramming. Environ. Exp. Bot. 157, 197–210.
Gong, Y., Chen, L.J., Pan, S.Y., Li, X.W., Xu, M.J., Qin, S., 2020. Antifungal potential evaluation and alleviation of salt stress in tomato seedlings by a halotolerant plant growth-promoting actinomycete Streptomyces sp. KLBMP5084. Rhizosphere 16, 100262.
Guerrieri, M.C., Fiorini, A., Fanfoni, E., Tabaglio, V., Cocconcelli, P.S., Trevisan, M., Puglisi, E., 2021. Integrated genomic and greenhouse assessment of a novel plant growth-promoting rhizobacterium for tomato plant. Front. Plant Sci. 12, 660620.
Guesmi, S., Mahjoubi, M., Pujic, P., Cherif, A., Normand, P., Sghaier, H., Boubakri, H., 2022. Biotechnological potential of *Kocuria rhizophila* PT10 isolated from roots of *Panicum turgidum*. Int. J. Environ. Sci. Technol. 19, 10105–10118.
Hackett, J.B., Shi, X., Kobylarz, A.T.M., Wessendorf, K.L.R.L., Hines, K.M., Bentolila, S., Hanson, M.R., Lu, Y., 2017. An organelle RNA recognition motif protein is required for photosystem II subunit psbF transcript editing. Plant Physiol. 173, 2278–2293.
Hayama, R., Yang, P., Valverde, F., Mizoguchi, T., Furutani-Hayama, I., Viestra, R.D., Coupland, G., 2019. Ubiquitin carboxyl-terminal hydrolases are required for period maintenance of the circadian clock at high temperature in *Arabidopsis*. Sci. Rep. 9, 17030.
Hoang, T.V., Vo, K.T.X., Rahman, M.M., Choi, S.H., Jeon, J.S., 2019. Heat stress transcription factor OsSPL7 plays a critical role in reactive oxygen species balance and stress responses in rice. Plant Sci. 289, 110273.
Jiao, P., Jin, S., Chen, N., Wang, C., Liu, S., Qu, J., Guan, S., Ma, Y., 2022. Improvement of cold tolerance in maize (*Zea mays* L.) using *Agrobacterium*-mediated transformation of ZmSAMDC gene. GM Crops Food 31, 131–141.
Kalt, W., 2005. Effects of production and processing factors on major fruit and vegetable antioxidants. J. Food Sci. 70 (1), R11–R19.
Ku, Y.S., Cheng, S.S., Cheung, M.Y., Lam, H.M., 2022. The roles of multidrug and toxic compound extrusion (MATE) transporters in regulating agronomic traits. Agronomy 12, 878.
La Rocca, G., King, B., Shui, B., Li, X., Zhang, M., Akat, K.M., Ogrodowski, P., Mastroleo, C., Chen, K., Cavalieri, V., Ma, Y., Anelli, V., Betel, D., Vidigal, J., Tuschl, T., Meister, G., Thompson, C., Lindsten, T., Haigis, K., Ventura, A., 2021. Inducible and reversible inhibition of miRNA-mediated gene repression in vivo. Elife 31, 70948.
Lan, G., Jiao, C., Wang, G., Sun, Y., Sun, Y., 2020. Effects of dopamine on growth, carbon metabolism, and nitrogen metabolism in cucumber under nitrate stress. Sci. Hortic. (Canterb.) 260, 304–4238.
Lephatsi, M.M., Meyer, V., Lizelle, A., PiaterIan, A., Dubery, Tugizimana, F., 2021. Plant responses to abiotic stresses and rhizobacterial biostimulants: metabolomics and epigenetics perspectives. Metabolites 11, 457.
Li, H., Liu, H., Wang, Y., Teng, R.M., Liu, J., Lin, S., Zhuang, J., 2020. Cytosolic ascorbate peroxidase 1 modulates ascorbic acid metabolism through cooperating with nitrogen regulatory protein P-II in tea plant under nitrogen deficiency stress. Genomics 112, 3497–3503.
Li, X., Sun, P., Zhang, Y., Jin, C., Guan, C., 2020. A novel PGPR strain *K. rhizophila* Y1 enhances salt stress tolerance in maize by regulating phytohormone levels, nutrient acquisition, redox potential, ion homeostasis, photosynthetic capacity and stress-responsive genes expression. Environ. Exp. Bot. 174, 104023.
Lin, Y., Sun, L., Nguyen, L.V., Rachubinski, R.A., Goodman, H.M., 1999. The pex16p homolog SSE1 and storage organelle formation in *Arabidopsis* seeds. Science 284, 328–330.
Liu, Q., Gao, T., Liu, W., Liu, Y., Zhao, Y., Liu, Y., Li, W., Ding, K., Ma, F., Li, C., 2020. Functions of dopamine in plants: a review. Plant Signal. Behav. 15, 1827782.
Lombardi, N., Caira, S., Troise, A.D., Scaloni, A., Vitaglione, P., Vinale, F., Marra, R., Salzano, A.M., Lorito, M., Woo, S.L., 2020. Trichoderma applications on strawberry plants modulate the physiological processes positively affecting fruit production and quality. Front. Microbiol. 3 (11), 1364.
Luo, J., Liu, M., Zhang, C., Zhang, P., Chen, J., Guo, Z., Lu, S., 2017. Transgenic centipedegrass (eremochloa ophiuroides [munro] hack.) overexpressing S-adenosylmethionine decarboxylase (SAMDC) gene for improved cold tolerance through involvement of H2O2 and NO signaling. Front. Plant Sci. 8, 1655.
Ma, Q., Liu, Y., Fang, H., Wang, P., Ahammed, G.J., Zai, W., Shi, K., 2020. An essential role of mitochondrial α-ketoglutarate dehydrogenase E2 in the basal immune response against bacterial pathogens in tomato. Front. Plant Sci. 11, 579772.
Micol-Ponce, R., Sarmiento-Mañús, R., Ruiz-Bayón, A., Montacié, C., Sáez-Vasquez, J., Ponce, M.R., 2018. *Arabidopsis* RIBOSOMAL RNA PROCESSING7 is required for 18S rRNA maturation. Plant Cell 30, 2855–2872.
Nebenführ, A., Dixit, R., 2018. Kinesins and myosins: molecular motors that coordinate cellular functions in plants. Annu. Rev. Plant Biol. 69, 329–361.
Nechushtai, R., Karmi, O., Zuo, K., Marjault, H.B., Darash-Yahana, M., Sohn, Y.S., King, S.D., Zandalinas, S.I., Carloni, P., Mittler, R., 2020. The balancing act of NEET proteins: iron, ROS, calcium and metabolism. Biochim. Biophys. Acta Mol. Cell Res. 1867 (11), 118805.
Puccio, G., Crucitti, A., Tiberini, A., Mauceri, A., Taglienti, A., Palumbo Piccionello, A., Carimi, F., van Kaauwen, M., Scholten, O., Sunseri, F., Vosman, B., Mercati, F., 2022. WRKY gene family drives dormancy release in onion bulbs. Cells 11, 1100.
Puccio, G., Ingraffia, R., Mercati, F., Amato, G., Giambalvo, D., Martinelli, F., Sunseri, F., Frenda, A.S., 2023. Transcriptome changes induced by Arbuscular mycorrhizal symbiosis in leaves of durum wheat (*Triticum durum* Desf.) promote higher salt tolerance. Sci. Rep. 13, 116.
Ray, P., Lakshmanan, V., Labbé, J.L., Craven, K.D., 2020. Microbe to microbiome: a paradigm shift in the application of microorganisms for sustainable agriculture. Front. Microbiol. 11, 622926.
Raza, A., Salehi, H., Rahman, M.A., Zahid, Z., Madadkar Haghjou, M., Najafi-Kakavand, S., Charagh, S., Osman, H.S., Albaqami, M., Zhuang, Y., Siddique, K.H.M., Zhuang, W., 2022. Plant hormones and neurotransmitter interactions mediate antioxidant defenses under induced oxidative stress in plants. Front. Plant Sci. 13, 961872.
Rey, P., Tarrago, L., 2018. Physiological roles of plant methionine sulfoxide reductases in redox homeostasis and signaling. Antioxidants 7, 114.
Rosina, M., Ceci, V., Turchi, R., Chuan, L., Borcherding, N., Sciarretta, F., Sánchez-Díaz, M., Tortolici, F., Karlinsey, K., Chiurchiù, V., Fuoco, C., Giwa, R., Field, R.L., Audano, M., Arena, S., Palma, A., Riccio, F., Shamsi, F., Renzone, G., Verri, M., Crescenzi, A., Rizza, S., Faienza, F., Filomeni, G., Kooijman, S., Rufini, S., de Vries, A. A.F., Scaloni, A., Mitro, N., Tseng, Y.H., Hidalgo, A., Zhou, B., Brestoff, J.R., Aquilano, K., Lettieri-Barbato, D., 2022. Ejection of damaged mitochondria and their removal by macrophages ensure efficient thermogenesis in brown adipose tissue. Cell Metabol. 34, 533–548.
Rouphael, Y., Colla, G., 2020. Editorial: biostimulants in agriculture. Front. Plant Sci. 11, 40.
Roy, S., Chakraborty, A.P., Chakraborty, R., 2021. Understanding the potential of root microbiome influencing salt-tolerance in plants and mechanisms involved at the transcriptional and translational level. Plant Physiol. 173, 1657–1681.
Ruzzi, M., Aroca, R., 2015. Plant growth-promoting rhizobacteria act as biostimulants in horticulture. Sci. Hortic. (Canterb.) 196, 124–134.
Sandalio, L.M., Rodríguez-Serrano, M., Romero-Puertas, M.C., del Río, L.A., 2013. Role of peroxisomes as a source of reactive oxygen species (ROS) signaling molecules. In: del Río, L. (Ed.), Peroxisomes and Their Key Role in Cellular Signaling and Metabolism, vol. 69. Subcell. Biochem.. Spr.
Shen, J., Zhao, Q., Wang, X., Gao, C., Zhu, Y., Zeng, Y., Jiang, L., 2018. A plant Bro1 domain protein BRAF regulates multivesicular body biogenesis and membrane protein homeostasis. Nat. Commun. 9, 3784.
Shu, K., Yang, W., 2017. E3 ubiquitin ligases: ubiquitous actors in plant development and abiotic stress responses. Plant Cell Physiol. 58 (9), 1461–1476.
Solis-Castañeda, G.J., Zamilpa, A., Cabañas-García, E., Marquina Bahena, S., Pérez-Molphe-Balch, E., Gómez-Aguirre, Y.A., 2020. Identification and quantitative determination of feruloyl-glucoside from hairy root cultures of *Turbinicarpus lophophoroides* (Werderm.) Buxb. & Backeb. (Cactaceae). In Vitro Cell Dev. Biol. Plant 56, 8–17.
Stackebrandt, E., Koch, C., Gvozdiak, O., Schumann, P., 1995. Taxonomic dissection of the genus Micrococcus: *K. rhizophila* gen. nov. Nesterenkonia gen. nov., Kytococcus gen. nov., Dermacoccus gen. nov., and Micrococcus cohn 1872 gen. Emend Int J Syst Evol Microbiol 45, 682–692.
Tassoni, A., Franceschetti, M., Tasco, G., Casadio, R., Bagni, N., 2007. Cloning, functional identification and structural modelling of *Vitis vinifera* S-adenosylmethionine decarboxylase. J. Plant Physiol. 164, 1208–1219.
Wang, Y., Perez-Sancho, J., Platre, M.P., Callebaut, B., Smokvarska, M., Ferrer, K., Luo, Y., Nolan, T.M., Sato, T., Busch, W., Benfey, P.N., Kvasnica, M., Winne, J.M., Bayer, E.M., Vukašinović, N., Russinova, E., 2023. Plasmodesmata mediate cell-to-cell transport of brassinosteroid hormones. Nat. Chem. Biol. 19, 1331–1341.
Wen, J., Jiang, F., Liu, M., Zhou, R., Sun, M., Shi, X., Zhu, Z., Wu, Z., 2021. Identification and expression analysis of Cathepsin B-like protease 2 genes in tomato at abiotic stresses especially at High temperature. Sci. Hortic. (Canterb.) 277, 109799.
Wiggins, G., Thomas, J., Rahmatallah, Y., Deen, C., Haynes, A., Degon, Z., Glazko, G., Mukherjee, A., 2022. Common gene expression patterns are observed in rice roots during associations with plant growth-promoting bacteria, *Herbaspirillum seropedicae* and *Azospirillum brasilense*. Sci. Rep. 12, 8827.
Xu, J.J., Fang, X., Li, C.Y., Zhao, Q., Martin, C., Chen, X.Y., Yang, L., 2018. Characterization of *Arabidopsis thaliana* hydroxyphenylpyruvate reductases in the tyrosine conversion pathway. Front. Plant Sci. 9, 1305.
Yang, J., Duan, G., Li, C., Liu, L., Han, G., Zhang, Y., Wang, C., 2019. The crosstalks between jasmonic acid and other plant hormone signaling highlight the involvement of jasmonic acid as a core component in plant response to biotic and abiotic stresses. Front. Plant Sci. 10, 1349.
Ye, J., Ding, W., Chen, Y., Zhu, X., Sun, J., Zheng, W., Zhang, B., Zhu, S., 2020. A nucleoside diphosphate kinase gene OsNDPK4 is involved in root development and defense responses in rice (*Oryza sativa* L.). Planta 251, 77.

Ye, Y., Ding, Y., Jiang, Q., Wang, F., Sun, J., Zhu, C., 2017. The role of receptor-like protein kinases (RLKs) in abiotic stress response in plants. Plant Cell Rep. 36 (2), 235–242.
Zhang, H., Lang, Z., Zhu, J.K., 2018. Dynamics and function of DNA methylation in plants. Nat. Rev. Mol. Cell Biol. 19, 489–506.
Zhou, Y., Sun, M., Sun, P., Gao, H., Yang, H., Jing, Y., Hussain, M.A., Saxena, R.K., Carther, F.I., Wang, Q., Li, H., 2022. Tonoplast inositol transporters: roles in plant abiotic stress response and crosstalk with other signals. J. Plant Physiol. 271, 153660.
Zhu, H., Tian, W., Zhu, X., Tang, X., Wu, L., Jin, S., 2020a. Ectopic expression of GhSAMDC1 improved plant vegetative growth and early flowering through conversion of spermidine to spermine in tobacco. Sci. Rep. 10, 14418.
Zhu, S., Estévez, J.M., Liao, H., Zhu, Y., Yang, T., Li, C., Wang, Y., Li, L., Liu, X., Pacheco, J.M., Guo, H., Yu, F., 2020b. The RALF1-FERONIA complex phosphorylates eIF4E1 to promote protein synthesis and polar root hair growth. Mol. Plant 13, 698–716.